

The Voltammetric Response of Nanometer-Sized Carbon Electrodes

Shengli Chen and Anthony Kucernak*

Department of Chemistry, Imperial College, London SW7 2AZ, U.K.

Received: March 28, 2002; In Final Form: June 26, 2002

Carbon electrodes of nanometer size have been fabricated by electrochemical etching of carbon fibers followed by deposition of electrophoretic paint. These electrodes have been characterized with steady-state voltammetry using a range of redox probes. These redox probes were chosen because they show a range of formal potentials and kinetic rate constants (k^0) and are charged to different extents. The voltammetric response of these electrodes in both the presence and absence of supporting electrolyte has been investigated. In the presence of supporting electrolyte, well-defined steady-state voltammograms of sigmoidal shape have been obtained on electrodes with effective radii as small as 1 nm. In the absence of supporting electrolyte, however, the voltammetric behavior varies with the redox system. Deviation from the expected migration–diffusion response is observed when the electrode is smaller than 20 nm for the reduction of the multicharged cationic species hexammineruthenium(III) ($\text{Ru}(\text{NH}_3)_6^{3+}$). Deviation from the ideal behavior of migration-coupled diffusion is exhibited at electrodes even of micrometer size during the reduction of the multicharged hexacyanoferrate(III) anion ($\text{Fe}(\text{CN})_6^{3-}$), which has a median reduction potential and relatively low k^0 . Such an effect is also observed for the oxidation of the hexacyanoferrate(II) anion ($\text{Fe}(\text{CN})_6^{4-}$). In comparison, the hexachloroiridate(IV) anion (IrCl_6^{2-}), with a higher k^0 and more positive reduction potential, shows deviations similar to those seen for hexammineruthenium(III); i.e., no deviation from expected behavior is seen until the electrode size is less than ca. 20 nm. It is argued that the dynamic diffuse double-layer effect rather than the Frumkin effect is the major source of the observed nonideal behavior. The results indicate that the dynamic diffuse double-layer effect can function even when the electrode reaction is reversible or quasi-reversible and becomes more pronounced at very small electrodes. The nature of size effects on the voltammetric response at nanometer size electrodes are discussed.

1. Introduction

Investigation of electrochemical phenomena using electrodes of submicrometer and nanometer size has been an attractive subject in electrochemical science since the late 1980s.^{1,2} The ultrasmall geometric dimension, high mass transport rate toward the electrodes and other features promise various novel applications of these electrodes, such as detecting single molecules,³ measuring the kinetics of fast electron-transfer reactions,^{2,4,5} probing neurochemical microenvironments,^{6–8} and scanning probe microscopy studies.^{9–11} In addition, the electrochemical behavior at electrodes of nanometer size generally exhibit deviation from the voltammetric theories of microelectrodes, hopefully leading to more precise and deeper understanding of the structure of the solid/liquid interface within nanodomains.¹² For example, Morris et al.¹ found that the limiting steady-state currents at band electrodes of width smaller than 10 nm were about an order of magnitude less than the value of limiting diffusion current predicated by the steady-state voltammetric theory of microelectrodes. The steady-state voltammetric response of nanometer electrodes in the absence of the supporting electrolyte were also found to differ from that expected from microelectrodes.^{13,14} In addition, the voltammetry at electrodes of nanometer size generally leads to considerable overestimation of the electron-transfer rate constant.^{2,4,15}

Despite the great attractiveness of nanometer-sized electrodes, results from such systems are actually rather rare. This is

probably due to the lack of any straightforward and reproducible ways for easy preparation of individual electrodes having very small electroactive areas. Fabrication of electrodes with extremely small electroactive area crucially depends on efficient coating methods, which allow insulation of the whole body except the very end of thinned tips of electrode materials. A number of coating materials have been used to produce submicrometer electrodes, including glass,^{2,4,9} nonconductive polymer film, nail varnish,^{16,17} wax,^{18,19} and electrophoretic paints.^{10,13,20} Much of this work was initiated to produce STM tips for use in electrochemical environments. Recently, several research groups have reported within the literature the fabrication of individual Pt electrodes having electrochemically active radii as small as several tens of nanometers, and even down to a few nanometers.^{2,4,13,20} Besides having extremely small electroactive areas, these electrodes showed a reliable voltammetric response, which is crucial in making electrochemical measurements. Compared to the procedures involving, for instance, translating etched metal tips through a molten glass bead at controlled speed² or the use of a laser micropipet puller,⁴ the method employing electrophoretic deposition of a polymer paint^{13,20} seems to be particularly straightforward and practical. It provides a relatively reproducible way to produce insulated electrodes of nanometer size.

Carbon has been an important electrode material in electroanalytical and electrocatalytic studies and applications due to its general availability, wide electrochemical window, and flexible surface properties through various chemical and electrochemical modifications. By employing electrochemical etch-

* Corresponding author. E-mail: a.kucernak@ic.ac.uk. Phone: +44 20 75945831. Fax: +44 20 75945804.

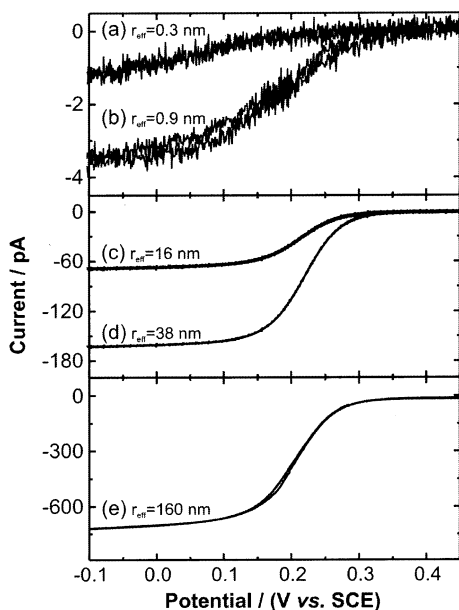


Figure 1. Steady-state cyclic voltammograms of reduction of $0.01 \text{ mol dm}^{-3} \text{ K}_3\text{Fe}(\text{CN})_6$ in the presence of $0.5 \text{ mol dm}^{-3} \text{ KCl}$ at carbon electrodes. $(dE/dt) = 0.010 \text{ V s}^{-1}$. The effective radii are calculated from limiting currents.

ing of carbon fibers followed by a novel new electrophoretic deposition process, we have recently reported the production of carbon electrodes having an effective radii as small as 1 nm.²¹ The new deposition approach for insulating the etched tips, the “inverted deposition” technique, allows for the simple and reproducible manufacture of such tips. In this paper, we present a detailed electrochemical characterization of the small carbon electrodes produced using this process. The voltammetric response of these electrodes on the reduction of hexacyanoferrate(III), hexachloroiridate(IV), and hexaammineruthenium(III), and the oxidation of hexacyanoferrate(II) have been investigated in the presence and absence of supporting electrolyte. In the presence of supporting electrolyte well-defined steady-state voltammetric responses have been obtained in these redox systems at electrodes with effective radii as small as 1 nm, Figure 1. However, in the absence of supporting electrolyte, the voltammetric response at very small electrodes shows significant deviation from the ideal behavior expected of such microelectrodes. Furthermore, such deviations are found to be dependent on (a) the electrode size, (b) reversibility of the redox system, and (c) charge of the redox molecule and its product. The results we obtain are interpreted in terms of the dynamic diffuse double-layer effect.

2. Experimental Section

Materials and Chemicals. The carbon fibers (PANEX33 CF, 95% carbon, unsized) were obtained from Zoltek Corp. Colloidal graphite (G303) was obtained from Agar Scientific Ltd. Cathodic electrophoretic paint (Clearclad HSR) was provided by LVH Coating Ltd. Chemicals (sources) used: $\text{K}_3\text{Fe}(\text{CN})_6$ (AnalaR BDH), $\text{K}_4\text{Fe}(\text{CN})_6 \cdot 3\text{H}_2\text{O}$ (AnalaR BDH), $\text{Ru}(\text{NH}_3)_6\text{Cl}_3$ (Aldrich, 98%), K_2IrCl_6 (Aldrich, 99.9%), methyl viologen (MV) (Aldrich, 98%), KCl (AnalaR, BDH), and NaOH (Aldrich). All solutions were prepared with Milli-Q water (Millipore, $18 \text{ M}\Omega \text{ cm}$).

Electrode Fabrication. A detail description of the electrode fabrication can be found in ref 21. After being thoroughly rinsed with ethanol and water respectively, the carbon fiber (5–6 mm in length and $3.6 \mu\text{m}$ in radius) was attached on one end of a

copper wire (0.5 mm radius) with a drop of colloidal graphite. After drying, the electrode was gently translated into an etching solution ($0.01 \text{ mol dm}^{-3} \text{ NaOH}$) with about 0.5–1 mm of the fiber immersed. An ac voltage (4–5 $\text{V}_{\text{p-p}}$, 50 Hz) was applied between the fiber and a graphite rod auxiliary electrode until the etching current falls to zero, typically requiring ca. 300 s. The fiber was then rinsed with water to remove any residual alkaline solution and left to dry prior to the insulation step.

The insulation of the etched tips involves two separate stages: electrophoretic deposition of paint onto the tip surface followed by a curing step at high temperatures to seal and harden the polymer insulation film. Shrinkage of the deposited film during the heating process is supposed to spontaneously expose the surface of the tip apex. We found that some complexities were involved in this insulation process. To be able to expose the tip end during the heating stage, a fairly thin paint layer has to be deposited on the fiber. Otherwise, a fully insulated electrode would be produced even after the subsequent heating stage. In contrast, if the coating layer is too thin, pinholes may be left in the film, some distance away from the tip, probably caused by slight roughness of the surface of the fiber. To overcome this difficulty, we have developed the so-called “inverted deposition” process. This technique involves inverting the fiber, so that the entire body of the electrode is immersed in the electrophoretic paint and then translating the fiber so that the tip just breaks through the solution surface.²¹ Thus, the tip apex only contacts with the solution via a very thin liquid meniscus, leading to virtually no deposition on the very apex, and an increase in deposition density as one moves away from the apex. After the heat cure process, we are left with an electrode with an exposed apex without any pinholes on the main fiber.

Deposition of electrophoretic paint was performed using a general dc power supply and a large graphite rod as the auxiliary electrode. Curing of the deposited film was performed at $\sim 195^\circ\text{C}$ for about 30 min. Repeated deposition and cure steps were performed to obtain smaller electrodes. A deposition voltage of 5–7 V applied for 60–90 s was employed in the first deposition and for 20–40 s in the following deposition steps. Predominantly, two or three deposition/heat cycles produce electrodes with electroactive radii of several tens of nanometers. For electrodes with effective radii of less than 10 nm, at least three deposition cycles are required. SEM images showed that the etched tips possessed a shallow tapered structure with a sharp end. The tip radii are at least below 50 nm. SEM images for the insulated tips with such a tiny electroactive area showed no clear interface between the polymer insulation and the exposed carbon fiber tip surface. This is probably due to the fact that both the electrode and coating materials have carbon as their principal component with the highest atomic number and thus show similar scattering efficiency. What can be seen from the SEM images of insulated tips is a smooth, defect-free insulation layer. A detailed characterization of these small carbon electrodes using electron microscopy is currently underway.

Electrochemical Measurements. An AutoLab PGSTAT20 potentiostat with the ECD module (Eco Chemie BV, Netherlands) was used in all electrochemical measurements. A two-electrode configuration with a calomel reference electrode as auxiliary separated from the working electrode through a Luggin capillary was employed in all voltammetric measurements. Pure argon was bubbled into solutions for at least 15 min before voltammetric measurements to remove any oxygen. An argon atmosphere above the solution was maintained during the measurements.

TABLE 1: Variation in $E_{1/2}$ and $|E_{3/4} - E_{1/4}|$ as a Function of Apparent Electrode Radius for a Carbon Ultramicroelectrode in 0.01 mol dm⁻³ K₃Fe(CN)₆ + 0.5 mol dm⁻³ KCl

r_{eff}/nm	$E_{1/2}/\text{V}$	$ E_{3/4} - E_{1/4} /\text{V}$
0.3	~0	
0.9	0.185	0.116
16	0.208	0.067
38	0.218	0.059
160	0.205	0.063

Throughout this paper, the electrode size quoted is actually an approximate estimation of the effective electroactive radii from the steady-state limiting current. Assuming that the exposed portion of the electrodes fabricated within this paper possess a hemispherical shape, then the diffusion-limited current is expected to follow²²

$$i_d = 2\pi nFDc_{\infty}r_{\text{eff}} \quad (1)$$

where D and c_{∞} are respectively the diffusion coefficient and the concentration of electroactive species in the electrolyte, r_{eff} is the effective radius of the electrode, and n is the number of electron involved in the electrode reaction. Thus, the value of r_{eff} can be determined from the measured steady-state limiting current in the presence of excess supporting electrolyte by using eq 1 with the known values of D , c_{∞} , and n . An example of the voltammetry of a range of electrodes of different sizes in 0.010 mol dm⁻³ Fe(CN)₆³⁻ + 0.5 mol dm⁻³ KCl is presented in Figure 1. Effective radii values were determined using the known diffusion coefficient²³ of Fe(CN)₆³⁻, 7.2×10^{-6} cm² s⁻¹. For electrodes with radii varying by almost 3 orders of magnitude both forward and reverse scans overlay each other almost exactly with virtually no hysteresis. Only at the smallest electrodes is there any indication of the distortion of the expected sigmoidal shape. For the smallest electrode, Figure 1a, the limiting current is ill-defined. The Tomes criteria ($|E_{3/4} - E_{1/4}|$), that is, the difference between the three-quarter wave potential and quarter wave potential, is close to 56 mV in the steady-state CVs obtained at electrodes 15 nm in radius and larger, Table 1. There also is a cathodic shift in the half-wave potential as the electrode decreases in size.

Estimates of electrode radius based on eq 1 assume a hemispherical geometry of the electrode and pure diffusional transport of the electroactive species in the solution; thus the values of r_{eff} quoted in this paper are only effective electroactive radii instead of the real electrode size. The real geometry of the electrodes may more likely be cone or hemispheroid. In addition, when the electrode size approaches values of molecular dimensions and/or the length of the electrical double layer, it is questionable whether the traditional transport and kinetic theories are an adequate description of the voltammetric behavior of such electrodes.¹² It has been generally realized that voltammetric analysis at such small electrodes may give considerable systematic errors in the determination of electron-transfer kinetics in the absence of reliable geometric information about the electrodes and accurate description of the transport of electroactive species.^{12b,24,25} In the present study, we have conducted investigations that compare the voltammetric response of these small electrodes in the absence and presence of supporting electrolyte. The conclusion should be qualitatively reliable because measurements in both the presence and absence of supporting electrolyte are performed on the same electrode.

3. Results

In the following sections we present the results of cyclic voltammetric measurement of redox probes at electrodes of different size in the presence and absence of a background electrolyte.

3.1. Reduction of Hexaammineruthenium(III). It has been shown that the reduction of hexaammineruthenium(III) (Ru(NH₃)₆³⁺) in the absence of supporting electrolyte at micrometer-sized electrodes can be well predicted by the recent theory in which the combined diffusion–migration of electroactive species is considered²⁶ (vide infra, eq 2). Our results indicate that even at electrodes down to around 20 nm, eq 2 is still applicable during the reduction of hexaammineruthenium(III). Figure 2 shows the steady-state voltammetric responses of carbon electrodes of various sizes on the reduction of 0.010 mol dm⁻³ Ru(NH₃)₆³⁺ in the presence and absence of supporting electrolyte (0.5 mol dm⁻³ KCl). The diffusion coefficient (D) of Ru(NH₃)₆³⁺ in KCl solution,²⁷ 8×10^{-6} cm² s⁻¹, was used to estimate the effective radii of electrodes (r_{eff}), which are indicated in the figures. In the presence of 0.5 mol dm⁻³ KCl, the reduction of hexaammineruthenium(III) shows a well-defined sigmoidal steady-state voltammetric response with almost perfect overlap of the forward and reverse sweeps even at electrodes having an effective radius of 1 nm. The Tomes criteria is close to 56 mV in the steady-state CVs obtained at electrodes larger than 50 nm, indicating that the electrode reaction is reversible. At electrodes of radii less than 10 nm, the CVs become significantly irreversible (Figure 2a,b). For example, the corresponding Tomes value is around 70–90 mV in the CV's obtained on electrodes with effective radii of 3 nm and 1 nm (electrical noise makes it difficult to determine this figure accurately). The half-wave potential value ($E_{1/2}$) shifts from -210 mV (large electrodes) to ca. -255 mV (3 nm) and -265 mV (1 nm), respectively.

In the absence of supporting electrolyte, well-defined sigmoidal steady-state CVs can be obtained at electrodes larger than 20 nm. Nonetheless, the half-wave potential shifts positively by about 30 mV in the absence of supporting electrolyte. When the electrode is smaller than 20 nm, the CV becomes gradually drawn out, and the corresponding half-wave potential shifts even more negative than that in the presence of supporting electrolyte. As can be seen in Figure 2a, almost no well-defined limiting current can be obtained when the electrode becomes very small. This seems to indicate that the electrode reaction becomes more irreversible in the absence of supporting electrolyte at such small electrodes; i.e., the apparent kinetic rate constant k_{app}^0 decreases.

3.2. Reduction of Hexacyanoferrate(III) and Oxidation of Hexacyanoferrate(II). The hexacyanoferrate redox couple (Fe(CN)₆^{3-/4-}) is generally accepted as a quasi-reversible redox couple with a kinetic rate constant of 0.14–0.18 cm s⁻¹ in KCl solution.^{27,28} Figure 1 gives the voltammetric response obtained for the reduction of 0.010 mol dm⁻³ Fe(CN)₆³⁻ in the presence of supporting electrolyte (0.5 mol dm⁻³ KCl) at carbon electrodes of different sizes. When the same electrodes were tested with both hexaammineruthenium(III) and hexacyanoferrate(III) it was noticed that the effective radii estimated from the limiting current in the presence of the latter redox probe is considerably smaller than the electrode size calculated for the former. For example, parallel experiments on the electrodes corresponding to Figure 1a,b on the reduction of 0.010 mol dm⁻³ Ru(NH₃)₆³⁺ with the same concentration of supporting electrolyte gave a steady-state limiting current that, especially for the smallest electrode, was significantly larger than that seen for the hexacyanoferrate(III) reduction. The ratio is strongly de-

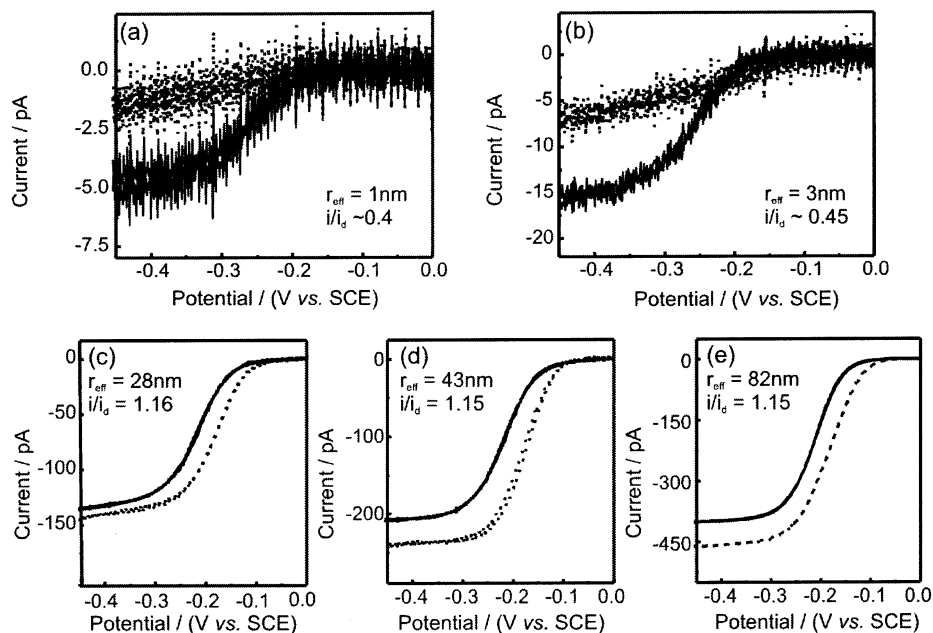


Figure 2. Steady-state cyclic voltammograms of the reduction of $0.01 \text{ mol dm}^{-3} \text{ Ru(NH}_3)_6\text{Cl}_3$ in the presence (—) and absence (···) of $0.5 \text{ mol dm}^{-3} \text{ KCl}$ supporting electrolyte at carbon ultramicroelectrodes. Indicated in the figures are the ratio between the limiting current (i) in the absence of $0.5 \text{ mol dm}^{-3} \text{ KCl}$ and the limiting current (i_d) in the presence of $0.5 \text{ mol dm}^{-3} \text{ KCl}$. The effective electroactive radii (r_{eff}) were calculated using eq 1 and i_d . $(dE/dt) = 0.010 \text{ V s}^{-1}$.

pendent on electrode size and disappears for electrodes as their radius approaches $1 \mu\text{m}$. These effects were much larger than might be expected from the difference in diffusion coefficient of the redox species. We found that the steady-state limiting current at the same electrode, taking into account D and c_∞ of each redox species, exhibits the following order for the reduction of a set of redox probes: $\text{Ru(NH}_3)_6^{3+} > \text{MV}^{2+} > \text{IrCl}_6^{2-} > \text{Fe(CN)}_6^{3-} \sim \text{Fe(CN)}_6^{4-}$. Such phenomenon may be due to the strong electrostatic interaction between the charged electrode and electroactive ions.¹² The effect of finite molecule size of electroactive ions may also play a significant role in this phenomenon when the critical dimension of the electrode becomes comparable to the size of molecules. At nanometer-sized electrode, the Boltzmann distribution law becomes questionable because it considerably overestimates the concentration of the counterion close to the electrode.^{1,29} It is predicted that at very small electrodes the strong interaction between the counterions and their finite size combine to decrease the concentration of the counterions near the OHP (outer Helmholtz plane) and therefore increases the extent of the diffuse double layer. We are currently investigating this effect and will report the results in a future paper. Although large errors may exist in the estimate of electrode size for small electrodes utilizing eq 1, these errors should not affect the qualitative conclusion in this paper.

According to the digital calculation by Smith et al.,¹² the reduction of negative charged ions such as hexacyanoferrate(III) should give a peaked current–potential curve. From the results shown here, it can be seen that well-defined sigmoidal steady-state voltammograms are actually maintained at very small electrodes (Figure 1a,b), but as described previously the limiting current appears to be strongly suppressed. A result of the depression of the limiting current is that the corresponding steady-state CV appears more reversible than the system really is. For instance, the CVs in Figure 1c,d look rather reversible although they are expected to be irreversible from the k^0 value of this couple.^{27,28}

Although even at very small electrodes the reduction of hexacyanoferrate(III) shows well-defined steady-state voltam-

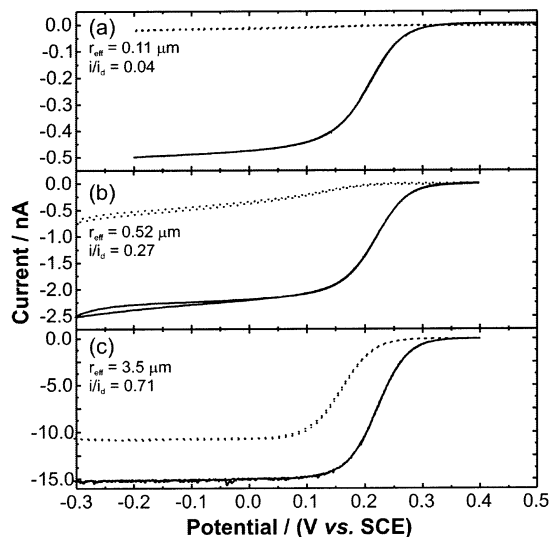


Figure 3. Steady-state cyclic voltammograms for the reduction of $0.01 \text{ mol dm}^{-3} \text{ K}_3\text{Fe(CN)}_6$ on carbon electrodes in the presence (—) and absence (···) of $0.5 \text{ mol dm}^{-3} \text{ KCl}$ supporting electrolyte. Indicated in the figures are the ratio between the limiting current (i) in the absence of $0.5 \text{ mol dm}^{-3} \text{ KCl}$ and the limiting current (i_d) in the presence of $0.5 \text{ mol dm}^{-3} \text{ KCl}$. The effective electroactive radii (r_{eff}) were calculated using eq 1 and i_d . $(dE/dt) = 0.010 \text{ V s}^{-1}$.

metric responses in the presence of supporting electrolyte, the corresponding voltammetric behavior in the absence of supporting electrolyte greatly deviates from what might be expected. For example, almost no reduction current can be observed at Pt microelectrodes having a radius of $5 \mu\text{m}$ in $0.001 \text{ mol dm}^{-3} \text{ Fe(CN)}_6^{3-}$ solution,²⁶ about 30% depression occurred in $0.005 \text{ mol dm}^{-3} \text{ Fe(CN)}_6^{3-}$ solution at a $6 \mu\text{m}$ radius Pt electrodes.³² Similar results were obtained on hexacyanoferrate(III) reduction at our carbon electrodes in $0.010 \text{ mol dm}^{-3} \text{ Fe(CN)}_6^{3-}$ solution. Furthermore, the extent of this inhibition strongly depends on the electrode size. This effect is illustrated in Figure 3, in which the cyclic voltammograms in the presence and absence of supporting electrolyte ($0.5 \text{ mol dm}^{-3} \text{ KCl}$) at electrodes of

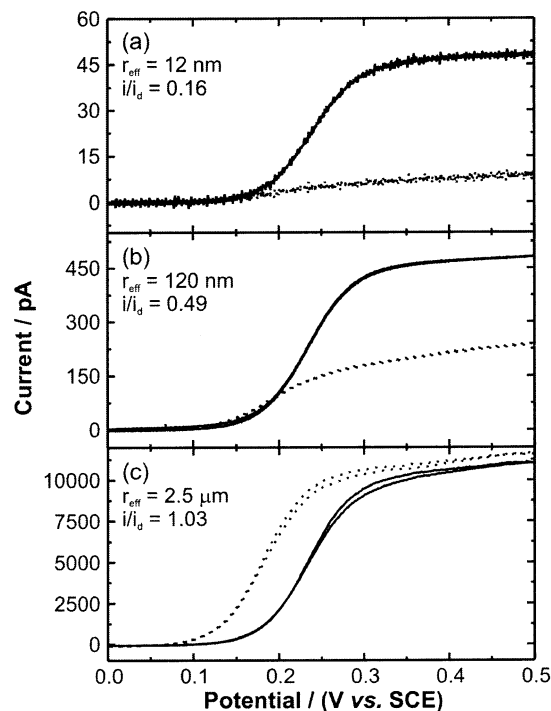


Figure 4. Steady-state cyclic voltammograms for the oxidation of $0.01 \text{ mol dm}^{-3} \text{ K}_4\text{Fe(CN)}_6$ in the presence (—) and absence (···) of $0.5 \text{ mol dm}^{-3} \text{ KCl}$ supporting electrolyte. Indicated in the figures are the ratio between the limiting current (i) in the absence of $0.5 \text{ mol dm}^{-3} \text{ KCl}$ and the limiting current (i_d) in the presence of $0.5 \text{ mol dm}^{-3} \text{ KCl}$. The effective electroactive radii (r_{eff}) were calculated using eq 1 and i_d . (dE/dt) = 0.010 V s^{-1} .

different size are shown. The forward and reverse scans overlap each other almost exactly. It can be seen that a decrease by more than 30% of the limiting plateau current occurs upon removal of the supporting electrolyte even on the electrodes with electroactive radius of around $3.5 \mu\text{m}$. At electrodes having radii of around 100 nm or less, a greater than 95% decrease in the reduction current was seen. Moreover, the steady-state voltammograms in the absence of supporting electrolyte become successively more ill defined as the electroactive radius of the electrode decreases.

As a comparison, the effect of the absence of supporting electrolyte on the oxidation of hexacyanoferrate(II) was also investigated. Figure 4 shows some typical cyclic voltammograms for the oxidation of $0.010 \text{ mol dm}^{-3} \text{ Fe(CN)}_6^{4-}$ in the presence and absence of $0.5 \text{ mol dm}^{-3} \text{ KCl}$ as a function of the size of the carbon microelectrode. The forward and reverse scans overlap each other almost exactly. At electrodes larger than $1 \mu\text{m}$, around a 3% enhancement of the limiting current occurs upon removal of supporting electrolyte. We see that significant inhibition of the electrode reaction occurs as the electrode becomes smaller. As shown in Figure 4b, the limiting current decreases by about 50% at electrodes for which r_{eff} is about 100 nm , when no supporting electrolyte is present. In comparison, for the reduction of hexacyanoferrate(III) similar inhibition rate occurs at electrodes of micrometer size. The degree of inhibition for hexacyanoferrate(III) reduction at electrodes of 100 nm size is more than 95%.

3.3. Reduction of Hexachloroiridate(IV). Hexachloroiridate(IV) (IrCl_6^{2-}) has a reduced negative charge and a more positive reduction potential than the hexacyanoferrate redox couple. The cyclic voltammograms corresponding to the reduction of hexachloroiridate(IV) in the presence and absence of supporting electrolyte at electrodes of three different sizes are shown in

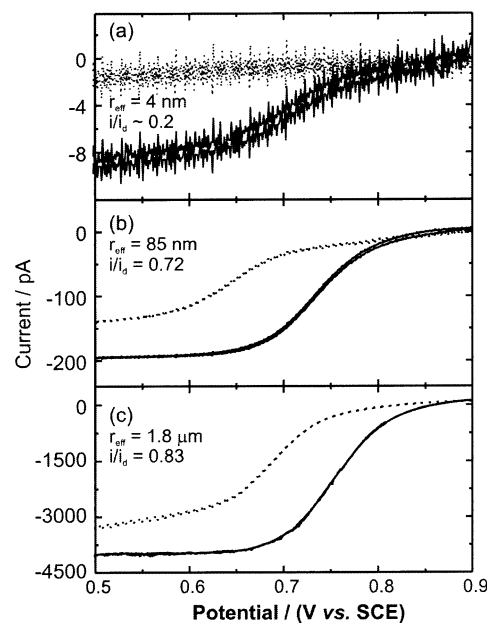


Figure 5. Steady-state cyclic voltammograms for the reduction of $0.005 \text{ mol dm}^{-3} \text{ K}_2\text{IrCl}_6$ in the presence (—) and absence (···) of $0.25 \text{ mol dm}^{-3} \text{ KCl}$ supporting electrolyte. Indicated in the figures are the ratio between the limiting current (i) in the absence of $0.25 \text{ mol dm}^{-3} \text{ KCl}$ and the limiting current (i_d) in the presence of $0.25 \text{ mol dm}^{-3} \text{ KCl}$. The effective electroactive radii (r_{eff}) were calculated using eq 1 and i_d . (dE/dt) = 0.010 V s^{-1} .

Figure 5. Because of the low solubility of K_2IrCl_6 , a concentration of $0.005 \text{ mol dm}^{-3}$ was used. Correspondingly, $0.25 \text{ mol dm}^{-3} \text{ KCl}$ was used as the supporting electrolyte to keep the ratio $c_{\text{redox}}/c_{\text{support}}$ constant. Surprisingly, a large potential shift between the voltammetric responses in the absence and presence of supporting electrolyte occurs for this redox couple.

For hexachloroiridate(IV) reduction, almost ideal behavior can be obtained on electrodes having micrometer size. As shown in Figure 5c, the limiting current decreases by about 17% upon removing the supporting electrolyte. As the electrodes become smaller, the CVs become gradually more irreversible and there is a greater depression of the limiting current in the absence of supporting electrolyte. Figure 5a shows the response at an electrode having an effective radius of 4 nm . Virtually no well-defined limiting current can be obtained, although the reduction current is still seen. It is clear that the reduction of hexachloroiridate(IV) exhibits a response that is more ideal than that for hexacyanoferrate(II) and hexacyanoferrate(III), although there is significant deviation from ideality at the smallest electrodes.

4. Discussion

The main purposes of adding excess inert electrolyte in “traditional voltammetry” is to form a compact electrical double layer, to suppress the electromigration of electroactive species and to increase the solution conductivity. Because the current is very small at microelectrodes, the resultant IR drop is usually very small. The other aspects of addition of supporting electrolyte, however, may not be neglected. In the following sections we discuss the likely effect of removing supporting electrolyte from our solutions

4.1. Electromigration Effects. In the presence of supporting electrolyte, the transport of the electroactive species is mostly through diffusion because the inert electrolyte ions carry the major portion of the migration current. However, if there is no excess inert electrolyte in the solution, the electroactive species reacting at the electrode/solution interface are transported by

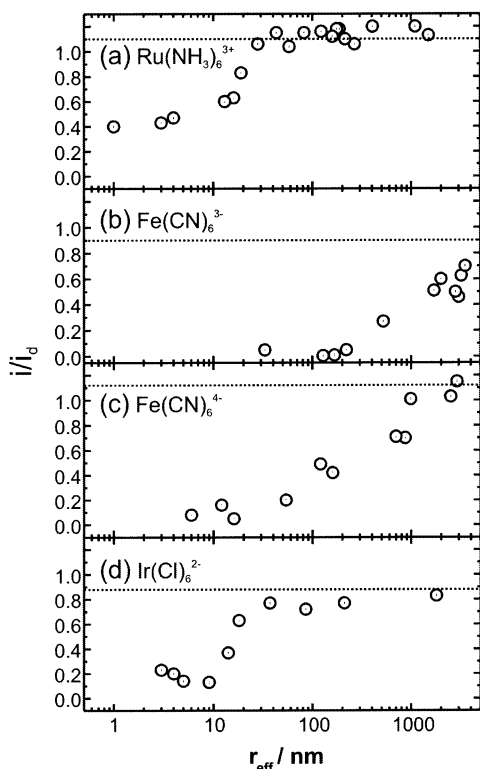


Figure 6. Variation in the ratio of limiting current in the presence (i_d) and absence (i) of supporting electrolyte ($0.5 \text{ mol dm}^{-3} \text{ KCl}$; $0.25 \text{ mol dm}^{-3} \text{ KCl}$ for K_2IrCl_6). Redox couples are present at a concentration of $0.010 \text{ mol dm}^{-3}$, except for K_2IrCl_6 ($0.005 \text{ mol dm}^{-3}$). The ratio calculated from theory (eq 2) is marked with a dotted line (---).

both diffusion and migration. The measured current thus consists of two contributions: the migration current and the diffusion current. There are a number of papers dealing with the migration effect on voltammetry at microelectrodes.^{30,31} Amatore et al.³¹ have derived a straightforward theoretical formulation to describe the relationship between the steady-state limiting current contributed by migration-coupled diffusion, i , and the limiting diffusion current, i_d :

$$\frac{i}{i_d} = 1 \pm z \left[1 + (1 + |z|)(1 - z/n) \times \ln \left(1 - \frac{1}{(1 + |z|)(1 - \{z\}/\{n\})} \right) \right] \quad (2)$$

where z is the charge of the electroactive ion and n (positive for reduction and negative for oxidation) is the number of electrons transferred in the electrode reaction. The sign (\pm) in this equation is positive for $n < z$ and negative for $n > z$. Equation 2 has been derived by assuming that the transport of the electroactive species is governed by the Nernst–Planck equation, that local electroneutrality is maintained, and that the electrode reaction is reversible. This equation has been found applicable or partially applicable to the voltammetric response seen for a range of redox couples at micrometer-sized electrodes.^{26,31}

In Figure 6 we summarize the results of a large number of experiments comparing the ratio of limiting current in the absence and presence of supporting electrolyte (i/i_d) for the previously mentioned redox probes as a function of r_{eff} . For very small electrodes ($r_{\text{eff}} < 5 \text{ nm}$) only an approximate value of i/i_d can be obtained, as no well-defined limiting current is reached in the absence of supporting electrolyte. In these cases the current value at the lower potential limit is used. Also

displayed in this diagram is the expected ratio of i/i_d calculated utilizing eq 2. In general, it can be seen that the ratio is only reached for relatively large electrodes and that for all redox couples the ratio tends toward small values at small r_{eff} . Furthermore, two different types of transition between “ideal” behavior (for which i/i_d is as expected) and “nonideal” behavior (for which i/i_d is much less than expected) are exhibited. For the case of hexaammineruthenium(III) and hexachloroiridate(IV) the transition occurs over a relatively narrow range of electrode sizes, whereas for the hexacyanoferrate couple, the transition occurs over ca. 2 orders of magnitude of electrode size.

When r_{eff} is larger than about 20 nm, the limiting current for the reduction of hexaammineruthenium(III) in the absence of supporting electrolyte is about 10% larger than that in the presence of supporting electrolyte. This is consistent with the prediction of eq 2, indicating that the reduction of hexaammineruthenium(III) is mainly governed by the migration-coupled diffusion process in the depletion layer at electrodes larger than 20 nm where the redox reaction is reversible or quasi-reversible. A significant dependence of i/i_d on r_{eff} occurs when the effective radius of electrode becomes less than or equal to 20 nm. The value of i/i_d shows a rapid decrease with r_{eff} and even becomes much less than 1 when $r_{\text{eff}} < 10 \text{ nm}$. This indicates that the assumptions used to derive eq 2 are no longer applicable for hexaammineruthenium(III) reduction at such small electrodes. For the reduction of hexachloroiridate(IV), Figure 6d, the deviation from expected behavior occurs over a similar range of r_{eff} . The limiting currents for hexachloroiridate(IV) reduction decrease by about 17% upon removing the supporting electrolyte for the largest electrode studied ($1.8 \mu\text{m}$), which is slightly more than the 12% reduction predicted by eq 2. For electrodes smaller than about 30 nm, significant deviations become obvious.

The situation for hexacyanoferrate(III) is much more extreme. According to the theoretical predictions of eq 2, there should be a depression of about 10% in the steady-state limiting plateau current of hexacyanoferrate(III) reduction upon removal of supporting electrolyte, whereas the actual depression is much larger for all electrodes studied. Such abnormal phenomenon was first observed by Lee et al.²⁶ on micrometer-sized electrodes. It was found that the depression depends on the electrode size and the concentration of the electroactive species.^{28,32} The oxidation of hexacyanoferrate(II) shows similar effects, although there is a shift toward smaller electrodes in the range over which the nonideal response takes hold.

4.2. Diffuse Double-Layer Effects. In dilute solution without excess inert electrolyte, there will be a considerable potential drop occurring in the diffuse part of the double layer. The potential drop across the diffuse double layer can significantly affect the measured current–potential curves. Such an effect is also called the “Frumkin effect” because of Frumkin’s pioneering analysis of this matter.³³ According to this analysis, the potential drop in the diffuse double layer affects the electrode reaction in two ways. On one hand, it modifies the concentration of redox ions at the plane of closest approach, which is usually assumed to be the outer Helmholtz plane (OHP, i.e., the end of the compact double layer on the solution side), according to the Boltzmann distribution law. Thus, the cation (anion) will be attracted to the OHP when the electrode is negatively (positively) charged and repelled from the OHP when the electrode is positively (negatively) charged. On the other hand, it modifies the value of the potential difference between the electrode and the OHP that drives the electron-transfer reaction. The former effect will either accelerate or slow the electrode

reaction depending on the charge properties of the electroactive species and the charge properties on the electrode surface. The latter effect will slow all the electrode reactions because it decreases the absolute value of the overpotential driving the reaction. The overall Frumkin effect will be an apparent change of the kinetic rate constant of the electrode reaction (k^0) with both applied potential and supporting electrolyte concentration.

According to traditional voltammetric theory, the Frumkin effect would only affect the kinetics of the charge-transfer process. If the electrode reaction is reversible, i.e., the electron-transfer rate is very fast compared to the mass transport rate, the concentration of electroactive species at the reaction plane is mainly governed by the slow transport process (migration and diffusion) in the depletion layer (diffusion layer) and the effect of the diffuse double layer is negligible. Thus, eq 2 can well predict the steady-state current at a microelectrode in the absence of supporting electrolyte because it is derived exactly on such an assumption.

When the electrode dimension becomes very small, the very high transport rate may exceed the rate at which reactant can be consumed at the surface. For example, at an electrode of 10 nm radius, a redox couple having a standard kinetic rate constant (k^0) of 10 cm s^{-1} can only produce quasi-reversible voltammetric responses for values of k^0/rD close to unity (assuming $D = 1 \times 10^{-5} \text{ cm}^2 \text{ s}^{-1}$).²² The k^0 value of the hexaammineruthenium couple is about 10 times less than 10 cm s^{-1} and might decrease another 5 times upon removal of supporting electrolyte.²⁷ Thus, the reduction of hexaammineruthenium(III) should be irreversible at electrodes smaller than 20 nm in the absence of supporting electrolyte and a strong Frumkin effect is expected to function. This might be the reason hexaammineruthenium(III) reduction in the absence of supporting electrolyte significantly deviates from eq 2 at small electrodes and the corresponding voltammograms become drawn out. At very small electrodes ($< 10 \text{ nm}$), a very strong Frumkin effect makes the limiting behavior unachievable. A similar approach may be used to rationalize the response seen in the presence of hexachloroiridate(IV). The kinetic rate constant for the hexachloroiridate couple is similar to that of the hexaammineruthenium couple.²⁷ So, we see similar effects predominating.

However, the actual effect of the absence of supporting electrolyte is much more complex than the analysis reviewed above. This can be indicated by the behavior of the hexacyanoferrate couple for which the reaction is reversible and eq 2 is only valid at electrodes of at least micron size. Nonideal voltammetric response in the absence of supporting electrolyte have been observed by Conyer et al.¹³ for the oxidation of ferrocenylmethylammonium hexafluorophosphate at insulated Pt electrodes of radius less than 10 nm. The voltammetric responses they obtained were quite reversible even at electrodes smaller than 10 nm. They speculated that the possible reason for nonideality at electrodes smaller than this was due to the dynamic diffuse double-layer effect, i.e., electrostatic influence on movement of charged reactant in the diffuse double layer.

4.3. Electroneutrality Assumption and the Dynamic Diffuse Double Layer. As mentioned above, the absence of supporting electrolyte can result in dramatic changes in the voltammetric responses that cannot be explained by eq 2 and the Frumkin effect. Equation 2 has been derived by assuming local electroneutrality and constant total concentration of various species in the depletion layer (i.e., the sum of the concentration of all species is invariant with distance) and with no consideration of the diffuse double layer.³¹ In reality, the diffuse double-layer potential drop is negligible only for two distinct situations:

either a concentrated electrolyte solution is used or the electrode potential is far away from the potential of zero charge (PZC). Under both of these conditions, the counterions compensating the charge on the electrode surface will be located mainly near the OHP and produce a very narrow diffuse double layer. As a result of this the potential drop mainly occurs in the compact layer. In dilute electrolytes, the diffuse double-layer effect is negligible only when the electrode potential is significantly different from the PZC. If the formal potential of a redox couple is close to the value of the PZC, it is expected that the voltammetric response will be greatly affected by the diffuse double layer.

Furthermore, electroneutrality in the depletion layer will not be maintained if there is an electric field present and a current flowing through the solution due to reaction at the electrode surface. When the current density is very small, one can expect that the deviation from electroneutrality is very small. And thus the assumption of electroneutrality will not result in significant error. However, when the current density is very high, there will necessarily be a nonequilibrium distribution of charged species in the depletion layer and thus local electroneutrality will not be maintained. The other assumption used in deriving eq 2, that the sum of concentrations of all species is distance independent, will also be invalid at high current densities. Therefore, we can predict that eq 2 will become invalid when the formal potential of a redox couple is close to the PZC value or the local current density at the electrode is very high.

As mass transport at small electrodes is enhanced, we expect to see higher current densities at smaller electrodes, with the current density scaling with $1/r$. Under these conditions it might be expected that there are significant local deviations from electroneutrality. In addition, when the electrode dimension approaches nanometer scales, i.e., comparable to both the length of the double layer and the molecular size of the electroactive species, other effects will also arise. As discussed previously, as the electrode radius decreases, the effects of ion-ion interaction and the exclusion volume effect (that is the volume excluded by each of the molecular species) will increase the length of the diffuse double layer. In contrast, the depletion layer of the microelectrode decreases with electrode size, as can be seen from the concentration distribution at microelectrodes of different sizes. Under pure diffusion control and assuming a spherical or hemispherical geometry of the electrode, the steady-state concentration distribution of electroactive species can be expressed as

$$c = c_\infty - \frac{r_0(c_\infty - c_0)}{r} \quad r \geq r_0 \quad (3)$$

$$\left(\frac{dc}{dr}\right) = \frac{r_0(c_\infty - c_0)}{r^2} \quad (4)$$

where r_0 is the radius of the electrode, and c_0 is the concentration of the electroactive species on the surface of the electrode. It can be seen that the concentration gradient will decrease to 1% of the value at r_0 at a distance of $10r_0$. Thus we can say that to a good approximation the length of the depletion layer will be $10r_0$. The simultaneous increase of diffuse double-layer length and decrease of depletion-layer length as the electrode radius decreases means that the extent of the overlap of the double layer with the depletion layer increases with decreased electrode size. This provides a further cause for electroneutrality to break down at smaller electrodes.

Frumkin analysis on the diffuse double layer is based on assumptions that there is a stationary and equilibrium charge

distribution in the diffuse double layer and the reaction plane is located at the OHP. In reality, dynamic charging of the diffuse double layer (i.e., dynamic distribution of charged reactants and products) may play an important role in the electrode reaction. The dynamic effect of the diffuse double layer³⁴ on the electrode reaction was first suggested by Levich in the 1940s³⁵ and recently has been more actively investigated.^{12,36} The equilibrium double-layer structure only describes the situation where there is no faradaic reaction occurring. If there is a faradaic current flowing through the cell, then the diffuse double layer is no longer stationary and at equilibrium. The movement, consumption, and production of charged ions will dynamically change the structure of the diffuse double layer. The high current density at the small electrode will thus make such dynamic effects of the diffuse double layer more pronounced.

As previously discussed, the Frumkin effect seems to be able to explain the nonideal behavior of the hexammineruthenium(III) reduction. However, as described in the last section, the first aspect of the Frumkin effect is actually beneficial to hexammineruthenium(III) reduction because the hexammineruthenium(III) cation would be attracted by the negatively charged electrode. The relatively strong inhibition of hexammineruthenium(III) reduction at very small electrodes thus seems to be unreasonable. This latter aspect can be understood in terms of the dynamic effect of the diffuse double layer. The production and accumulation of another cation, e.g., hexammineruthenium(II), would offset the negative potential of the diffuse double layer and repel the reactant. Such dynamic effects render the overall effect of the diffuse double-layer disadvantageous to the electrode reaction.

Very similar results to hexammineruthenium(III) reduction (not shown here) have been obtained on the reduction of methyl viologen (MV^{2+}). Ideal responses consistent with eq 2 can be obtained when the effective radius is not less than 20 nm. No extra enhancement of the reduction current has been observed, although the reduction of methyl viologen occurs at more negative potential. The diffuse double-layer effect may enhance those electroreduction processes of cations that produce neutral species.

Such a strong inhibition of hexacyanoferrate(III) reduction in the absence of supporting electrolyte, as seen in Figure 3, even at electrodes of several micrometers cannot be reasonably explained by the Frumkin effect. The k^0 value of the hexacyanoferrate redox system is about 5 times lower than that for the hexammineruthenium couple.^{27,28} Thus it is expected that a strong Frumkin effect should occur when the electrodes have effective radii of 100 nm or less. At microelectrodes, hexacyanoferrate(III) reduction is actually rather reversible. The variation of response with electrode size may be more easily understood when the dynamic charging of the diffuse double layer is considered. It is expected that anions such as hexacyanoferrate(III) will be repelled in the diffuse double layer during the reduction process. Furthermore, the production of more negatively charged hexacyanoferrate(II) tends to shift the diffuse-layer potential more negative so that the reactant is strongly repelled from approaching the reaction plane (OHP) and the effective overpotential is greatly offset. In a recent asymptotic analysis, Bonnefont et al.^{36a} showed that the dynamic diffuse double effect could be very strong even at a large electrode when the k^0 of the system is low and the length of the diffuse layer is comparable to or larger than that of the compact layer. The actual limiting current in the system might be a reaction-limited current that is much smaller than the limiting diffusion current. Similar results were obtained by

digital simulation of microelectrode voltammetry by Norton et al.^{12a} The reduction of hexacyanoferrate(III) seems to belong to such a case. The irreversibility of the electrode reaction increases with a decrease of electrode size; therefore the diffuse double-layer effect becomes more pronounced at smaller electrodes.

At an electrode of 10 nm size the current for the oxidation of hexacyanoferrate(II) is still seen in the absence of the supporting electrolyte (Figure 4c). The results of hexacyanoferrate(II) oxidation seem to confirm the inhibition mechanism of dynamic diffuse-layer effect on the reduction of hexacyanoferrate(III). The limiting current in the oxidation of hexacyanoferrate(II) occurs at more positive potential than the hexacyanoferrate(III) reduction; the corresponding diffuse double layer would be more amenable toward the oxidation process. However, the diffuse double layer still seems to repel the hexacyanoferrate(II) anion because removing the supporting electrolyte suppresses hexacyanoferrate(II) oxidation. The production of hexacyanoferrate(III) during the oxidation favors a negative diffuse-double layer, therefore decreasing the approach of reactant to the reaction plane. This is similar to hexammineruthenium(III) reduction at very small electrodes discussed in the last section.

Other sources may also be involved in the strong effect of diffuse double layer on the hexacyanoferrate redox systems. This redox couple has a relatively median formal potential, which might be close to the zero charge potential at which the diffuse double-layer effect is more pronounced. In addition, the blockage effect due to surface adsorption of reactant decomposition products may also contribute to the inhibition occurring in the hexacyanoferrate redox system.^{27,28} However, there is a shift in the inhibition plots, Figure 6b,c, for these two species, implying that the inhibition cannot solely be due to such a chemical effect, for which identical curves would be expected. If the adsorbed species were some kind of anion, then the diffuse double-layer potential would be much more negative and the reactant anions thus strongly repelled. In the absence of supporting electrolyte, the excess cation can stabilize the reactants from decomposition.²⁷ The present data are not able to confirm such speculations.

It should be emphasized here that the electrode size data we have presented only have qualitative rather than quantitative significance because considerable error may be involved in determining the electrode size from limiting current for very small electrodes. Another point that may have some bearing on the voltammetric response of these electrodes is that the functional groups on the carbon surface have complex charge properties and their coverage are variable with electrode potential. Such variation of surface properties with potential may very well affect the double-layer structure and offset or enhance the properties of the electrode toward a given electron-transfer reaction. In addition, the electrical double layer surrounding the coating layer of electrophoretic paint may also affect the double-layer structure of the carbon electrode.

5. Conclusion

The voltammetric responses of carbon nanometer electrodes have been investigated using redox systems with different charge properties, formal potential, and kinetic rate constant (k^0) in the presence and absence of supporting electrolyte. Well-defined steady-state voltammograms of sigmoidal shape have been obtained in the presence of supporting electrolyte at electrodes having effective electroactive radii as small as 1 nm. In the absence of supporting electrolyte, the voltammetric responses

of these electrodes are found to depend on the specific properties of the redox system and the electrode size. For the reduction of multicharged cations such as hexaammineruthenium(III) and MV^{2+} , which have a negative formal potential and high k^0 , the voltammetric responses are controlled mainly by the diffusion and migration of electroactive species in the depletion layer (diffusion layer) if the effective radius of electrode is larger than 20 nm. Such an effect is also exhibited for the reduction of hexachloroiridate(IV), an ion with a rather positive formal potential but with a similar k^0 value to $Ru(NH_3)_6^{3+}$. Although the reduction of hexacyanoferrate(III) and oxidation of hexacyanoferrate(II) show well-defined steady-state voltammetric responses in the presence of supporting electrolyte and at nanometer-sized electrodes, in the absence of supporting electrolyte nonideal behavior, which greatly deviates from that expected, is exhibited. Such nonideality also occurs in other redox systems at electrodes of much smaller size and has been interpreted in terms of dynamic changes within the diffuse double layer. At smaller electrodes the high current density is expected to lead to a significant deviation from the condition of local electroneutrality, and this too is expected to have a significant effect on the diffuse double layer. The effect of the diffuse double layer depends on the electrode size and the formal potential of the redox couple.

Acknowledgment. This research has been made possible by support from the Leverhulme trust (Grant number F/07058C). Mr. Peter Hope from LVH Ltd. is thanked for kindly providing the electrophoretic paint solution and making many helpful suggestions on its use. Mr. Simon Turner is thanked for his workshop skills.

References and Notes

- (1) Morris, R. B.; Franta, D. J.; White, H. S. *J. Phys. Chem.* **1987**, *91*, 3559.
- (2) Penner, R. M.; Heben, M. J.; Longin, T. L.; Lewis, N. S. *Science* **1990**, *250*, 1118.
- (3) (a) Fan, F.-R. F.; Bard, A. J. *Science* **1995**, *267*, 871. (b) Fan, F.-R. F.; Kwak, J.; Bard, A. J. *J. Am. Chem. Soc.* **1996**, *118*, 9669.
- (4) Shao, Y.; Mirkin, M. V.; Fish, G.; Kokotov, S.; Palanker, D.; Lewis, A. *Anal. Chem.* **1997**, *69*, 1627.
- (5) Bowyer, W. J.; Engelman, E. E.; Evans, D. H. *J. Electroanal. Chem.* **1989**, *262*, 67.
- (6) Giros, B.; Jaber, M.; Jones, S. R.; Wightman, R. M. *Nature* **1996**, *379*, 606.
- (7) Kuras, A.; Gutmaniene, N. *J. Neurosci. Methods* **2000**, *96*, 143.
- (8) Chien, J. B.; Wallingford, R. A.; Ewing, A. G. *J. Neurochem.* **1990**, *54*, 633–638.
- (9) Heben, M. J.; Dovek, M. M.; Lewis, N. S.; Penner, R. M.; Quate, C. F. *J. Microscopy* **1988**, *152*, 651.
- (10) (a) Bach, C. E.; Nichols, R. J.; Meyer, H.; Besenhard, J. O. *Surf. Coat. Technol.* **1994**, *67*, 139. (b) Bach, C. E.; Nichols, R. J.; Beckmann, W.; Meyer, H.; Schulte, A.; Besenhard, J. O. *J. Electrochem. Soc.* **1993**, *140*, 1281. (c) Mao, B. W.; Ye, J. H.; Zhuo, X. D.; Mu, J. Q.; Fen, Z. D.; Tian, Z. W. *Ultramicroscopy* **1992**, *42*, 464.
- (11) (a) Lee, C.; Miller, C. J.; Bard, A. J. *Anal. Chem.* **1991**, *63*, 78. (b) Macpherson, J. V.; Unwin, P. R. *Anal. Chem.* **2000**, *72*, 276–285.
- (12) (a) Norton, J. D.; White, H. S.; Feldberg, S. W. *J. Phys. Chem.* **1990**, *94*, 6772. (b) Smith, C. P.; White, H. S. *Anal. Chem.* **1993**, *65*, 3343.
- (13) Conyers, J. L.; White, H. S. *Anal. Chem.* **2000**, *72*, 4441.
- (14) Menon, V. P.; Martin, C. R. *Anal. Chem.* **1995**, *67*, 1920.
- (15) Chen, J. Y.; Aoki, K. *Electrochem. Commun.* **2002**, *4*, 24.
- (16) Groen, M. P.; Hanson, K. J.; Scherson, D. A.; Xing, X.; Richter, M.; Ross, P. N.; Carr, R.; Lindau, I. *J. Phys. Chem.* **1989**, *93*, 2181.
- (17) Vitus, C. M.; Chang, S. C.; Schardt, B. C.; Weaver, M. J. *Phys. Chem.* **1991**, *95*, 7558.
- (18) Wiechers, J.; Twomey, T.; Kolb, D. M.; Behm, R. J. *J. Electroanal. Chem.* **1988**, *248*, 451.
- (19) (a) Nagahara, L. A.; Thundat, T.; Lindsay, S. M. *Rev. Sci. Instrum.* **1989**, *60*, 3128. (b) Mirkin, M. V.; Fan, F.-R. F.; Bard, A. J. *J. Electroanal. Chem.* **1992**, *328*, 47.
- (20) Slevin, C. J.; Gray, N. J.; Macpherson, J. V.; Webb, M. A.; Unwin, P. R. *Electrochem. Commun.* **1999**, *1*, 282.
- (21) Chen, S. L.; Kucernak, A. *Electrochem. Commun.* **2002**, *4*, 80.
- (22) Montenegro, M. I.; Queiros, M. A.; Daschbach, J. L. *Micro-electrodes: Theory and Applications*; Kluwer Academic Press: Dordrecht, The Netherlands, 1991.
- (23) Kawagoe, K. T.; Jankowski, J. A.; Wightman, R. M. *Anal. Chem.* **1991**, *63*, 1589–1594.
- (24) Baranski, A. S. *J. Electroanal. Chem.* **1991**, *307*, 287.
- (25) Oldham, K. B. *Anal. Chem.* **1992**, *64*, 646.
- (26) Lee, C.; Anson, F. C. *J. Electroanal. Chem.* **1992**, *323*, 381.
- (27) Beriet, C.; Pletcher, D. J. *Electroanal. Chem.* **1994**, *375*, 213.
- (28) Beriet, C.; Pletcher, D. J. *Electroanal. Chem.* **1993**, *361*, 93.
- (29) Fawcett, W. R. *J. Electroanal. Chem.* **2001**, *500*, 264.
- (30) (a) Oldham, K. B. *J. Electroanal. Chem.* **1988**, *250*, 1. (b) Myland, J. C.; Oldham, K. B. *J. Electroanal. Chem.* **1993**, *347*, 49.
- (31) (a) Amatore, C.; Fosset, B.; Bartlet, J.; Deakin, M. R.; Wightman, R. M. *J. Electroanal. Chem.* **1988**, *256*, 255–268. (b) Amatore, C.; Deakin, M. R.; Wightman, R. M. *J. Electroanal. Chem.* **1987**, *220*, 49–63.
- (32) Rooney, M. B.; Coomber, D. C.; Bond, A. M. *Anal. Chem.* **2000**, *72*, 3486.
- (33) Bard, A. J.; Faulkner, L. R. *Electrochemical Methods*; John Wiley: New York, 1980.
- (34) Actually, the so-called dynamic diffuse double-layer effect is merely a more accurate description of the Frumkin effect—they are not two independent effects.
- (35) Levich, B. *Dokl. Akad. Nauk SSSR* **1949**, *67*, 309.
- (36) (a) Bonnefont, A.; Argoul, F.; Bazant, M. Z. *J. Electroanal. Chem.* **2001**, *500*, 52. (b) Murphy, W. D.; Manzanarez, J. A.; Mafé, S.; Reiss, H. *J. Phys. Chem.* **1992**, *96*, 9983.